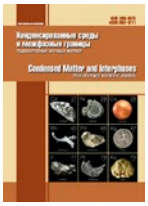

ISSN 1606-867X (Print)
ISSN 2687-0711 (Online)
Condensed Matter and Interphases
Kondensirovannye Sredy i Mezhfaznye Granitsy
https://journals.vsu.ru/kcmf/

Original articles

Research article
https://doi.org/10.17308/kcmf.2024.26/12428

Phase transformations of ternary copper iron sulfide $Cu_{1.1}Fe_{1.9}S_{3.0}$ under temperature variations: thermodynamic and kinetic aspects

I. G. Vasilyeva[1]✉, E. F. Sinyakova[2], S. A. Gromilov[1]

[1]Nikolaev Institute of Inorganic Chemistry of Siberian Branch Russian Academy of Sciences
3 Lavrent'ev ave., Novosibirsk 630090, Russian Federation

[2]VS Sobolev Institute of Geology and Mineralogy Siberian Branch Russian Academy of Sciences
pr. Akademika Koptyuga 3, Novosibirsk, 630090, Russian Federation

Abstract

The article considers ternary sulfide $Cu_{1.1}Fe_{1.9}S_3$ with a metal/sulfur ratio corresponding to the complete stoichiometry of cubanite $CuFe_2S_3$ as an intermediate phase of a solid solution with chemically disordered Cu and Fe cations in the ordered anionic framework. A new approach to determining the nature of the solid solution, its stability and behavior during cooled over a wide temperature and time range is suggested. To synthesize the sample, we used controlled directional solidification of a homogeneous melt with the $Cu_{1.1}Fe_{1.9}S_3$ composition under quasi-equilibrium conditions and obtained a solidified zoned ingot, where the distribution of Cu, Fe, and S elements along its length was quantitatively determined. To detect small-scale structural and chemical changes, we used optical and electron microscopy methods, electron-probe X-ray spectral microanalysis, full-profile X-ray diffraction analysis, and the differential dissolution method, which allowed to determine the phase and chemical states of the samples both at the macro level and with a high spatial resolution. With this approach, we established the following: $Cu_{1.1}Fe_{1.9}S_3$ is an intermediate phase of a system with end-members of cubanite $CuFe_2S_3$ and chalcopyrite $CuFeS_2$; a homogeneous solid solution of chalcopyrite with 5 mol. % of cubanite exists near 930 °C with a chaotic distribution of Cu and Fe between the existing crystallographic positions; a solid solution of chalcopyrite with 6 mol. % of cubanite at 900 °C facilitates lattice strain relaxation through the formation of a block nanostructure; there is a solid solution of cubanite with 30 mol. % of chalcopyrite at 900–720 °C, with small-size clusters with a chalcopyrite stoichiometry evenly distributed inside the $Cu_{0.94}Fe_2S_3$ matrix. The factors determining the evolution and stability of solid solutions are discussed taking into account the polymorphism of chalcopyrite phase. The newly obtained data is important for the synthesis of magnetic nanosized Cu-Fe sulfide materials and can also be used in the processing of sulfide ores rich in copper.

Keywords: System Cu-Fe-S, Directional Crystallization, Solid Solutions, Ordering

Funding: The research was carried out with the financial support of the Ministry of Science and Higher Education of the Russian Federation under the Government Order by Nikolaev Institute of Inorganic Chemistry of the Siberian Branch of the Russian Academy of Sciences (agreement No. 121031700315-2) and V.S. Sobolev Institute of Geology and Mineralogy of the Siberian Branch of the Russian Academy of Sciences (agreement No. 122041400237-8).

Acknowledgements: Scanning electron microscopy and energy-dispersive spectrometry (SEM/EDS) studies were performed at the Centre for Collective Use of Multielement and Isotope Studies of the Siberian Branch of the Russian Academy of Sciences.

For citation: Vasilyeva I. G., Sinyakova E. F., Gromilov S. A. Phase transformations of ternary copper iron sulfide $Cu_{1.1}Fe_{1.9}S_{3.0}$ under temperature variations: thermodynamic and kinetic aspects *Condensed Matter and Interphases*. 2024;26(4): 706–715. https://doi.org/10.17308/kcmf.2024.26/12428

Для цитирования: Васильева И. Г., Синякова Е. Ф., Громилов С. А. Фазовые превращения тройного сульфида железа-меди $Cu_{1.1}Fe_{1.9}S_{3.0}$ при варьировании температуры: некоторые термодинамические и кинетические аспекты. *Конденсированные среды и межфазные границы*. 2024;26(4): 706–715. https://doi.org/10.17308/kcmf.2024.26/12428

✉ Inga G. Vasilyeva, e-mail: kamars@niic.nsc.ru
© Vasilyeva I. G., Sinyakova E. F., Gromilov S.A., 2024

The content is available under Creative Commons Attribution 4.0 License.

1. Introduction

Ternary sulfides $CuFe_2S_3$ and $CuFeS_2$, especially nanosized, have recently attracted a lot of attention due to their magnetic and semiconductor properties, which make them promising materials for the development of information technologies [1-3]. Being the main minerals of sulfide ores rich in copper, they are also the main source of non-ferrous metals [4–6]. Both sulfides are formed in a similar way, namely by means of melt crystallization followed by solid-phase transformations of the crystallized product during the cooling process. In this regard, cubanite $CuFe_2S_3$ and chalcopyrite $CuFeS_2$ are unique compounds that besides stable polymorphic phases they have a large number of metastable structural forms with the Cu and Fe cations distribution depending on the cooling kinetics [4–6]. Such a diversity of structures ensures as well the variability of the properties of ternary sulfides. Therefore, an understanding of the evolution of solid-phase processes is very important both for the purposeful synthesis of new materials and for the development of efficient technologies for the processing of mineral associations.

The existing knowledge about cubanite and chalcopyrite transformations is mainly based on the results of numerous studies of natural minerals, which are final products of crystallization, whereas synthetic analogues are used to determine their intermediate states through annealing- quenching procedure. At the moment, there is plenty of data regarding the transformation of low-temperature orthorhombic cubanite $CuFe_2S_3$ (*Pcmn a* = 6.46 Å, *b* = 11.12 Å, *c* = 6.23 Å) into a high-temperature cubic polymorph ($F\bar{4}3m$ *a* = 5.29 Å). It is known that the reverse transition is kinetically inhibited and cannot be implemented in laboratory experiments. Under nature conditions, on the contrary, the association of orthorhombic cubanite – chalcopyrite is stable with reaching equilibrium at 300–400 ºC during 1–10 years [4, 5]. An alternative to polymorphic transition, a metastable process of the tetragonal chalcopyrite exsolution from cubanite was found [4, 7-10] or tetragonal chalcopyrite with iron monosulfide according to the following reaction: $CuFe_2S_3 \rightarrow CuFeS_2 + FeS$ [11]. These processes are usually studied using electron probe microanalysis (EPM) and X-ray diffraction analysis of the microstructures of the minerals and their analogues. Nevertheless, according to references [1, 4, 9–10], serious limitations of these diagnostic methods, and long-term isothermal annealing of tetragonal chalcopyrite at temperature close to the equilibrium 300–400 ºC, makes practically impossible studying of high-temperature small-scale order-disorder transformations with participation of high-temperature cubic chalcopyrite. A high-temperature chalcopyrite polymorph with a completely cation-disordered cubic structure ($F\bar{4}3m$ *a* = 5.29 Å) was discovered during an *in situ* experiment with transmission electron microscopy (TEM) [12, 13]. The critical temperature 557 °C was determined for the phase transition of the tetragonal $CuFeS_2$ → cubic $CuFeS_2$ using a combination of methods, including neutron powder and X-ray diffraction, thermal analysis, and magnetic and electron transport measurements. It is important that this temperature is characteristic only for the strictly stoichiometric composition of both these phases [11, 14]. Since phase transformations of cubic chalcopyrite – cubic cubanite at high temperatures depend on the stoichiometry of the interacting phases, these experiments aimed should be carefully designed. When the symmetry and the lattice parameters of both these phases are identical, efficient methods should be used to identify chalcopyrite in cubanite mixtures, especially when it occurs in a dispersed state in the cubic cubanite matrix. So, cubanite, cooled from high temperatures in *the in-situ* TEM experiment, contained lamellae with isolated finely dispersed particles, but its diffraction picture was absolutely identical to the initial one [15]. Unfortunately, for study of the order-disorder transformations of ternary Cu-Fe sulfides, abilities of TEM experiments are hindered both the difficulty in preparing the samples and even more so by the radiation causing a loss of sulfur and therefore changes in the characteristics of themselves transformations. Therefore, to study high-temperature transformations of a solidified $Cu_{1.1}Fe_{1.9}S_3$ melt, a new synthesis and new diagnostic methods of small-scale structural changes were used. A sample was obtained in the form of an ingot during conservative directional

crystallization and the solidified melt passed across zones with lowered temperatures over various periods of time. The calculation of the qualitative distribution of Cu, Fe, and S along the ingot length gave data regarding the Cu/Fe ratio in the each moment of crystallization and the bulk compositions varying along the length. The crystallization method is described in [16, 17], its efficiency for the study of exsolution process of stoichiometric cubanite $CuFe_2S_3$ is demonstrated in [20]. Fragments of equilibrium *T-x* diagrams in the range adjacent to $CuFe_2S_3$ and $Cu_{1.1}Fe_2S_3$ compositions were shown in [18, 19]. To study fine structure transformations, the reference-free differential dissolution method (DD) was used along with traditional methods. It reliably identified phases having identical structures but different compositions and internal arranging, based on differences in their chemical activity. The principles of the DD method is given in [21, 22] with its abilities to identify unknown, amorphous, or low-dimensional phases based on their composition without referring to the phase standards. And it is an advantage over the X-ray diffraction method (XRD), especially when the analyzed samples have a complex spatial arrangement. Scanning composition with a resolution of 5Å/cm^2, DD method determines the spatial chemical inhomogeneity of the phase, caused difference of its internal arrange, and like this practically substitutes for TEM, which registers this arrange structurally.

2. Experimental

Directional crystallization of the melt with a composition Fe 32.5, Cu 18.5, S 49.0 at. % was performed using the Bridgman-Stockbarger method with moving the ampoule with the homogeneous melt from the hot area to the cold area at $2.3 \cdot 10^{-8}$ m/s and its quenching in air at ~ 100 deg/min, when the temperature at its end reached 720 °C. As known, this cooling procedure practically corresponds to the natural equilibrium crystallization of minerals [5]. The ingot, 70 mm long and 7 mm in diameter, was cut into 14 wafers. Based on the results of the analysis of these wafers, we practically obtained a kinetic time-temperature-transformation diagram. Changes in the morphology, phase and chemical states of the polished wafers were registered by means of step-wise scanning of the surface using optical and electron microscopy. The average (scanning area of ~2 mm^2) and local chemical compositions of components with different morphology and geometry were measured using the methodology developed at the Centre for Collective Use of Multielement and Isotope Studies of the Siberian Branch of the Russian Academy of Sciences by means of energy-dispersive spectrometry (SEM-EDS) on a MIRA 3 LMU high-resolution microscope (Tescan Orsay Holding) equipped with INCA Energy 450+ X-Max 80 and INCA Wave 500 (Oxford Instruments Nanoanalysis Ltd) microanalysis systems. The error in determining the main components was 0.1–0.3 wt.%. The compositions of ~ 5 μm particles of different phases were determined based on single measurements with a relative error of 1-2%.

The XRD was performed using a Shimadzu XRD-7000 powder diffractometer at 20 ºC, Cu*K*α-radiation, range 20–75° 2θ, scan rate of 0.1 °/min, standards Si and LaB_6. After abrasion, thin layers of the sample were put on the polished side of a standard cuvette. The phases were identified using ICSD No. 42105 for $CuFe_2S_3$, No. 28894 for $CuFeS_2$, and No. 42487 for FeS [23]; a full-profile analysis of the X-ray diffraction patterns was performed using the Powder Cell program [24].

In the DD experiment (Fig. 1a), the consequent dissolution of phases was realized in a solvent flow with the concentration gradually increasing from 3N HNO_3 at 40 °C to 6N HNO_3 at 85 °C. Phases with different chemical potentials dissolve consequently once their potentials equal the potential of the solvent. The solvent was fed to the reactor in portions at a constant speed. Each portion with a dissolved 5Å surface layer of the sample then came to an ICP-AES spectrometer, which simultaneously determined amounts of Cu, Fe, and S. Kinetic curves of dissolution of the components and their stoichiograms, presented as pairwise atomic ratios of the components of this sample, were obtained based on the analysis of 50–200 portions of the solution. The computer-processed primary data was used to determine the number of phases, their compositions, quantities, and spatial homogeneity, and it was demonstrated by dissolving a model phase mixture $A_2B_3 + AB_3$ (Fig. 1b).

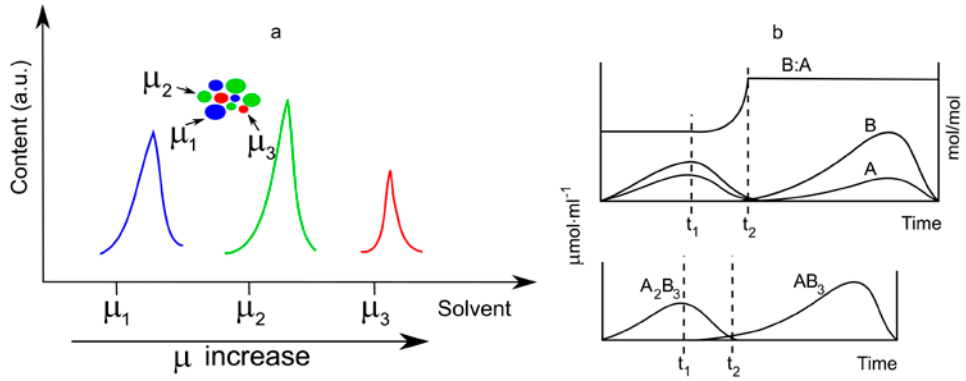

Fig. 1. Principles of DD: consecutive dissolution of phases according to chemical potentials μ (a); dissolution of the model phase mixture A_2B_3 + AB_3(b): A, B – kinetic curves of A and B elements dissolution and stoichiogram line B:A (top); kinetic curves of dissolution of the A_2B_3 и AB_3 phases (bottom)

3. Results and discussion

In [6], the fragmentary equilibrium *T-x* diagram $Cu_{0.19}Fe_{0.33}S_{0.48}$ - $Cu_{0.31}Fe_{0.23}S_{0.46}$ of the Cu-Fe-S system is shown (Fig. 2) where the phase of a constant composition $Cu_{1.1}Fe_{1.9}S_{3.0}$ was considered as a nonstoichiometric cubanite (*icb**) being in equilibrium with the melt. However, there are two facts indicating a different nature of this sulfide. The first is a partial cationic substitution of iron with copper, without deviation of the metal/sulfur ratio from generally 2/3 stoichiometry. The second, known from [5, 6], is the ability of the high-temperature cubic solid solution *iss* of the Cu-Fe-S ternary system to interact with chalcopyrite of the same structure. A reconstruction of elementary composition of $Cu_{1.1}Fe_{1.9}S_{3.0}$ to crystallochemical composition $CuFe_{1.73}S_{2.73}$ reflects a novel nature of the phase where the cationic substitution happens in the anionic framework of cubanite remaining unchanged. The chemical disorder results in the formation of substitutional solid solutions with variable contents of Cu and Fe. From the point of view of crystal chemistry, the composition $CuFe_{1.73}S_{2.73}$ is defined as an intermediate solid solution with the $0.73CuFe_2S_3 \cdot O.27CuFeS_2$ composition, where the end-members are cubanite and chalcopyrite. The purpose of our study was to gather evidence of the nature of the solid solution and determine its stability and behavior over a wide temperature during cooling.

Fig. 3 demonstrates the cooling regime of the ingot, i.e. a kinetic diagram of high-temperature subsolidus transformations of the solidified $Cu_{1.1}Fe_{1.9}S_{3.0}$ melt. According to macrostructure, the ingot has three obviously differ zones. We focused on zones II and III, where the numbers in the figure correspond to the wafers cut from the ingot. It is easy to see the duration of stay of the samples in each temperature field. Micrographs of the surface of the polished wafers in an optical and electron microscopes are given in Fig. 4. The microstructure of the 0.56 sample was typical for all the samples in zone II, microstructures of samples 0.96 and 1.0 in zone III were different from each other and from the samples in zone II. Optical microscopy demonstrated that all the samples, except for 0.96, are single-phase at the macro level according to the uniformity of their color and reflectivity. Sample 0.96 includes light and dark domains of various size,

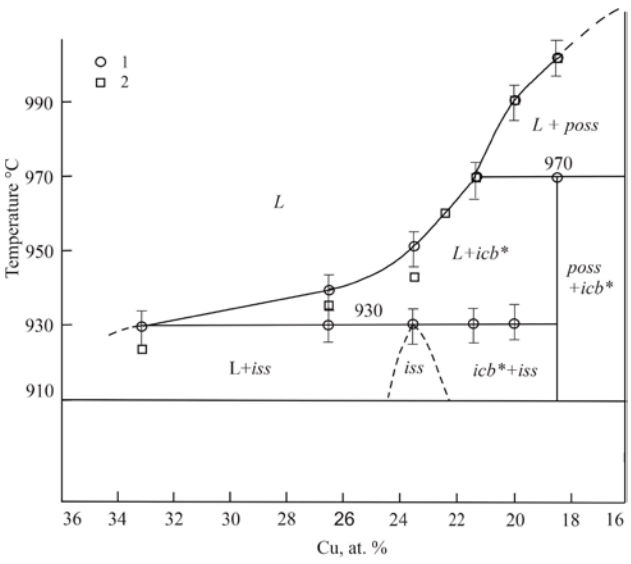

Fig. 2. Polythermal section along the $Cu_{0.19}Fe_{0.33}S_{0.48}$ - $Cu_{0.31}Fe_{0.23}S_{0.46}$ direction [19]. *L* – sulfide melt, *poss* – $(Fe,Cu)S_{1.04}$, *icb** – $Cu_{1.1}Fe_{2.0}S_{3.0}$, and *iss* – $Cu_{1.0}Fe_{1.2}S_{2.0}$

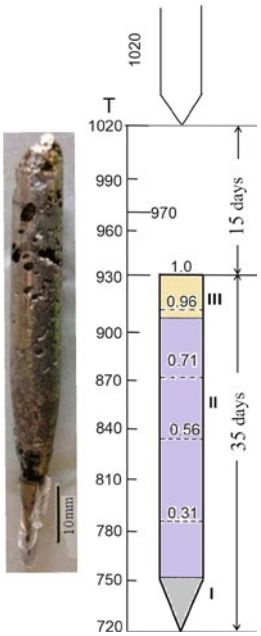

Fig. 3. View of ingot (left) and kinetic diagram (right)

and the difference in color is explained by the difference in their compositions and internal arranges (Fig. 4b, c). Microstructure of all the samples from SEM observation did not shown diffraction contrast as well as lamellae, rims, or microinclusions being visible signs of exsolution process (Fig. 4e-i). The high accuracy of the average composition of wafers due to a large wealth of EDX data obtained by EDS, and the sum of the determined concentrations of the components practically equal to 100 %, make it possible to reconstruct the bulk composition into a corresponding crystallochemical formula.

Table 1 presents bulk and crystallochemical compositions of the samples. It shows that compositions of the samples in zone II are kept constant but different from 0.96 and 1.0 samples in zone III. There is only a slight difference between the latter two compositions. According to crystallochemical formulas, in zone II a cubanite-based solid solution with 30 mol. % of chalcopyrite is realized; in zone III a solid solution of chalcopyrite with 5 or 6 mol. % of cubanite is formed. What formation of these solid solutions is realistic fact is supported by their homogeneous microstructures.

The single-phase state of the representative specimens 0.31–0.71, 0.96, and 1 was emerged

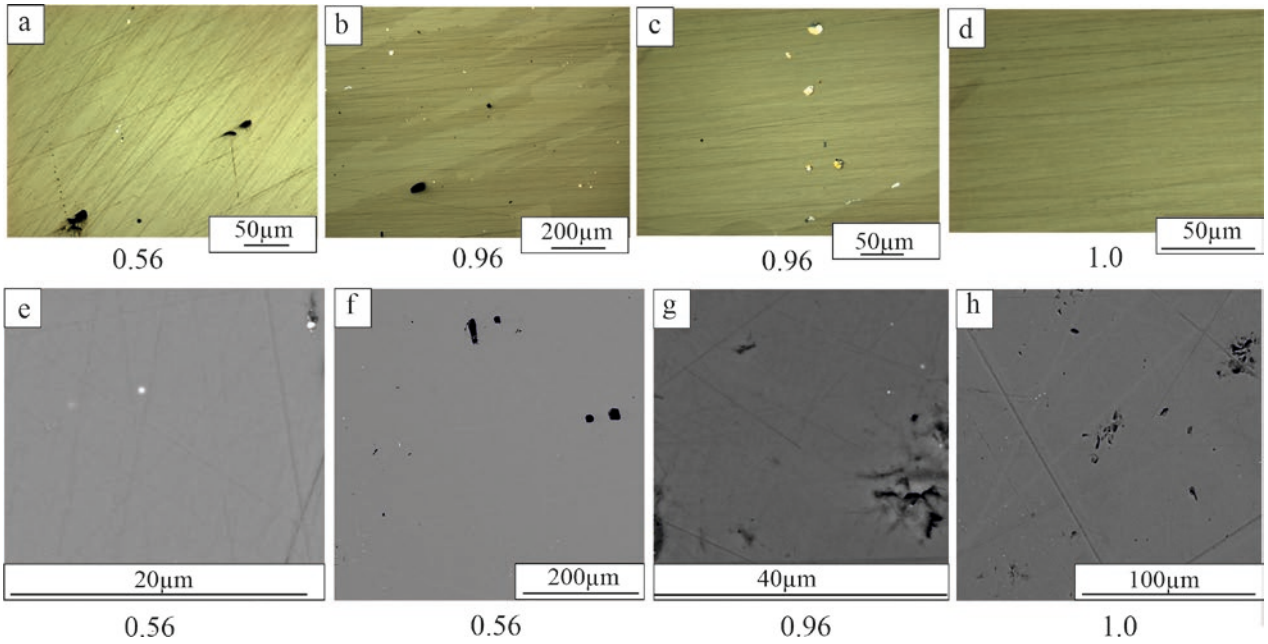

Fig. 4. Microstructure of samples 0.56, 0.96 and 1.0 in reflected light (a-d) and in BSE (e-h)

Table 1. Variation of average composition along the ingot length in zones II and III

Samples	0.31	0.56	0.71	0.83	0.95	0.96	1.0
Состав	$CuFe_{1.73}S_{2.6}$	$CuFe_{1.73}S_{2.6}$	$CuFe_{1.73}S_{2.6}$	$CuFe_{1.73}S_{2.6}$	$CuFe_{1.73}S_{2.6}$	$CuFe_{1.20}S_{2.08}$	$CuFe_{1.18}S_{2.05}$
Solid solutions	$0.7CuFe_2S_3 \cdot 0.3CuFeS_2$					$0.95CuFeS_2 \cdot 0.05CuFe_2S_3$	

also from a diffraction experiment (Table 2). Quite reproducible diffraction patterns, taking from various parts of the samples 0.56, 0.96, and 1.0, with full-profile analysis showed the same type of cubic structure $F\bar{4}3m$ (Fig. 5). The only difference was observed in the lattice parameter and a specific change in the relative intensity of the diffraction peak (220). The largest lattice parameter was observed for sample 1.0. For samples 0.96 and 0.56, it decreased, becoming the lowest in the part of the 0.96 sample that adjacent to the boundary of zone III. Changes in the lattice parameter of cubic cubanite are usually associated with the presence of microdistortions deforming the lattice [8–10, 25, 26]. In our experiment, changes in the lattice parameters caused significant changes in the Cu:Fe ratio and therefore changes in the manner of their distribution between corresponding crystallographic positions. A peculiar profile of the peak (220), namely broadening of the pedestal, is typical of samples in zone II with the boundary part of the 0.96 sample. Since this peculiarity can be caused by various local structure distortions, reliability of X-ray diffraction data was ensured by the results of the DD method, which performs also the phase analysis through differential dissolution of the representative specimens. Kinetic curves of the Cu, Fe, and S elements dissolution of the 1.0 sample shows only one peak and the Cu:Fe

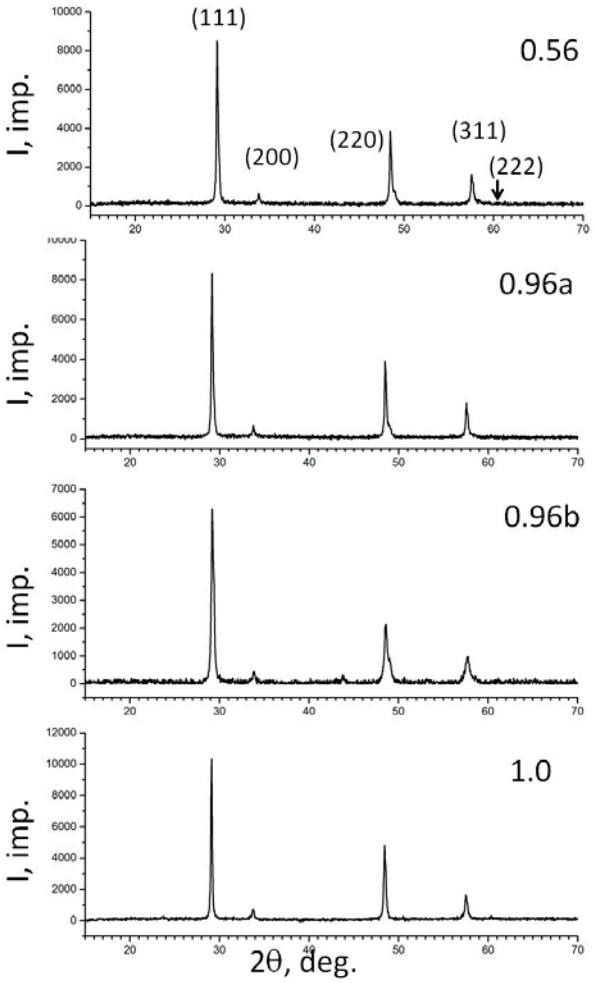

Fig. 5. Difractograms of powder samples 0.56, 0.96a, 0.96b and 1.0

Table 2. Structural parameters of samples 0.56, 0.96 and 1.0

	111	200	220	311*
Sample 0.56 (a = 5.307 Å)				
2q	29.126	33.757	48.470$_{дв}$**	57,549
d_{exp}, Å	3.063	2.653	1.877	1.600
FWHM, °	0.18	0.19	0.19	0.21
Sample 1.0 (a = 5.312 Å)				
2q	29.089	33.719	48.422	57.498
d_{exp}, Å	3.067	2.656	1.878	1.602
FWHM, °	0.13	0.20	0.20	0.24
Sample 0.96a (a = 5.307 Å)				
2q	29.121	33.738	48.478$_{дв}$**	57.555
d_{exp}, Å	3.064	2.655	1.876	1.600
FWHM, °	0.17	0.19	0.17	0.18
Sample 0.96б (a = 5.298 Å)				
2q	29.197	33.802	48.570$_{дв}$**	57.659
d_{exp}, Å	3.056	2.649	1.873	1.597
FWHM, °	0.29	0.29	0.44	0.54

* Line used for determination of the unit cell parameter. ** Double line.

stoichiogram is linear, equals 0.84 and remains constant during the full dissolution of the sample. The quantities of Cu and Fe together with the S quantity, gives a chemical formula $CuFe_{1.19}S_2$ of this spatially homogeneous phase with the content of 94±4 wt. % (Fig. 6b). The 0.96 sample dissolves also as a single phase with the content of 92±4 wt. %. However, the kinetic curve of the elements dissolution demonstrates three peaks, and a linear Cu:Fe stoichiogram gradually changes the initial value 0.85 to 0.81 at the end of the dissolution process (Fig. 6a). The deduced composition as $CuFe_{1.20\text{-}1.23}S_2$ reflects the chemical inhomogeneity of this phase caused by blocks of various compositions. Sample 0.56 has another bulk composition ($CuFe_{1.78}S_{2.7}$) and dissolves in a different manner. Its kinetic curves have several peaks, and Cu:Fe stoichiogram involves two linear fragments of various length: the first fragment, plotted on 30 experimental points, was $Cu_{0.8\pm0.1}Fe_1$, the second, $Cu_{0.47\pm0.04}Fe_1$ was plotted on 114 points (Fig. 7a). Both fragments, recalculated into chemical formula, indicate the presence of the stoichiometric cubanite as main phase (83 wt. %) and stoichiometric chalcopyrite as impurity nanoparticles (13 wt. %), i.e. an ordered structure. Here, composition is a reliable dignostic sign of the phase for the chalcopyrite nanoparticles, but the DD method cannot determine the size, shape, and the particle–matrix interface. However, location of the chalcopyrite peak inside the cubanite peak on the kinetic curves and the observed chemical variability of each portion of the solution, dissolving thin surface layer of the sample, mean that chalcopyrite particles are uniformly dispersed in the cubanite matrix.

Summarized diagnostic data of the samples 0.56, 0.96, and 1 allowed to present the sequence of the solidified melt transformations under cooling conditions. Sample 1.0 with a bulk composition $CuFe_{1.19}S_{2.04}$ crystallized from the melt with a ratio Cu/Fe = 0.71 and rather quickly cooled down at temperatures close to 930 °C; according to the spatial resolution of the used diagnostic methods, it is a uniform, chemically and structurally homogeneous phase based on $CuFeS_2$ with composition moved towards $CuFe_2S_3$ by 5 mol. % within the homogeneity range. At a higher resolution, a quasi-homogeneous state with associations can be found. Earlier, when the cubic chalcopyrite had not yet been identified, the homogeneous state of $0.7{\cdot}CuFeS_2 + 0.3{\cdot}CuFe_2S_3$ at high temperatures was identified as a tetragonal chalcopyrite phase enriched with iron [25]. This means that studying the mechanisms of solid-phase transformations of Cu-Fe sulfide phases presents severe problems caused by the lack of key data for correctly interpret thin phase and chemical changes.

Sample 0.96 of the bulk composition $CuFe_{1.21}S_{2.07}$ with chemically different domains that are not registered on diffraction patterns, demonstrates the initial stage of the ordering process with Cu and Fe cations, occupying topologically inequivalent positions in the cubic structure. According to the kinetic diagram

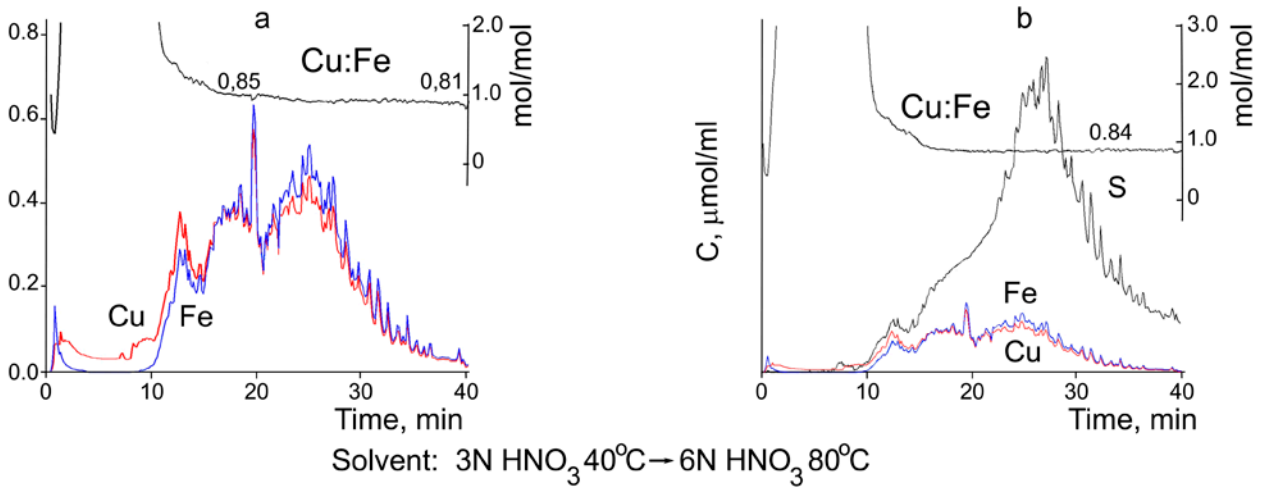

Fig. 6. Kinetic curves of Cu, Fe, S elements dissolution for samples 0.96 (a) and 1.0 (b)

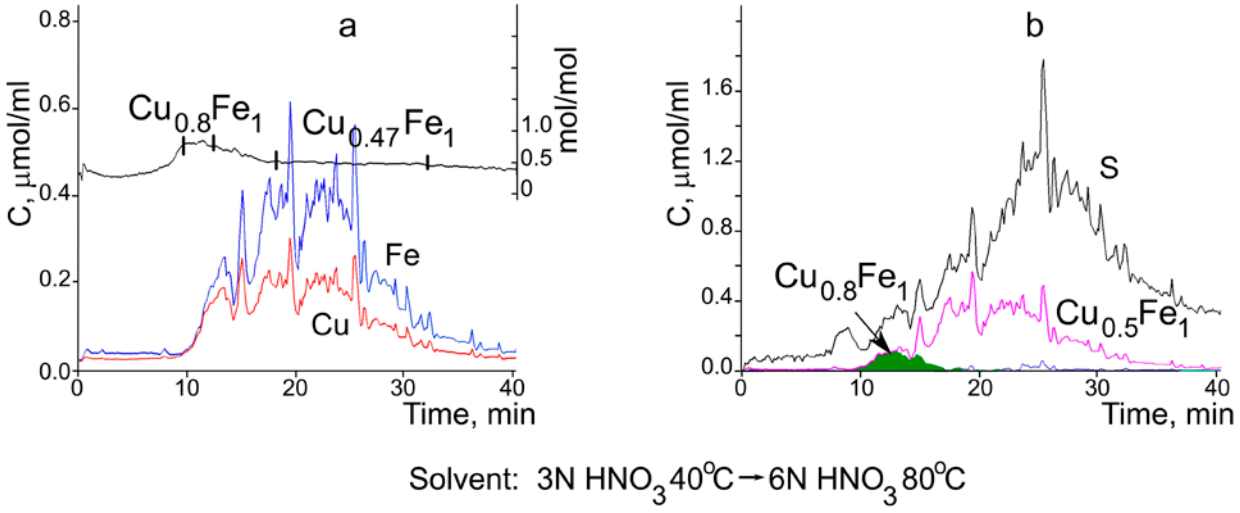

Fig. 7. Kinetic curves of Cu, Fe, S elements dissolution and linear dashes fragments of stoichiograms Cu:Fe (a); kinetic curves of chalcopyrite and cubanite dissolution (b)

(Fig. 3), formation of this state took a long period of time required for the migration of cations through the sulfide lattice. This is the early stage of decomposition of the solid solution, which is usually allusive and cannot be detected due to small-scale changes of this homogeneous solid solution. This stage is associated with the ordering of cations without changing the structure, but with altering the bonds length depending on the distribution of multi-charge cations with similar radii (Cu_4^{+1} = 0.74Å, Fe_4^{+3} = 0.77Å). The changes in the lattice parameter of sample 0.96 relative the parameter of sample 1.0 are demonstrated in Table 2. Finding the early ordering stage is of crucial importance, because a new internal structural arrange of the ordered state forms also other physico-chemical properties and thus other characteristics of the polymorphic transition from cubic chalcopyrite to tetragonal.

Sample 0.56, homogeneous in its reflectivity and diffraction properties, is heterogeneous at micro level according to the DD results: the cubanite matrix contains low-dimensional chalcopyrite clusters occurring in specific lattice centers. According to a TEM experiment, the size of such dispersed formations exsoluted from cubanite during its cooling from the highest temperatures is several nm [3, 15]. In our experiment, the small size of the clusters indicated the inhibition of the nucleation and growth processes. That is why the SEM experiment did not reveal any signs of decomposition of the solid solution in all the samples of the II zone, even those that were cooled for a long time at lower temperatures, Fig. 4. These clusters escape detection by X-ray diffraction, but their appearance caused changes in the interplanar distances resulting in a broadening of the peak (220). The nature of the peak broadening was discussed in [8, 9, 14, 26, 27]. Most authors agree that this phenomenon is associated with the formation of intergrowth structures of cubanite with chalcopyrite: the peak with d = 1.862, which is characteristic for pure cubanite, is laid over a peak with d = 1.878, corresponding to the intergrowth structure. We believe that clusters of cubic chalcopyrite form tense microstructures with the cubic matrix, thus increasing the unit cell volume. This metastable state remains even after long-term annealing at 400 °C, i.e. in the field of stability of tetragonal chalcopyrite, Fig. 4f. The stability of this solid solution is also confirmed by two other well-known facts: adding cubanite to chalcopyrite reduces the temperature of its polymorphic transition from 570 to 400 °C [26]; kinetic inhibition of the reconstructive polymorphic transition of chalcopyrite proceeds very slowly and gradually following the ordering of the cubic structure and desymmetrization of type $F\bar{4}3m \rightarrow P\bar{4}3m \rightarrow I\bar{4}3m \rightarrow P\bar{4}2m$ [12].

As a result, we obtained justified and agreed data regarding the early decomposition stages of

the $Cu_{1.1}Fe_{1.9}S_{3.0}$ solid solution. The decomposition is initiated by cationic ordering with the formation of domains with various compositions and internal structural arrange without interrupting the interface surface. This is followed by the decomposition and formation of a nanostructure of two coexisting cubic phases of chalcopyrite and cubanite, which is stable over a wide temperature range, metastable, and apparently coherent.

4. Conclusions

In this article, we suggested a new methodological approach for solving a complex task of determining nature of the initial stages of transformations of the intermediate phase $Cu_{1.1}Fe_{1.9}S_{3.0}$ of cubic solid solution during cooling. In our experiment, we focused on the development of diagnostic methods that can determine the texture changes, composition, and structure of the samples with a high spatial resolution in function of thermodynamic and kinetic cooling conditions. This allowed us to understand the process, which includes stages of cationic ordering followed by the formation of a metastable solid solution of nanosized clusters of cubic chalcopyrite in the cubic cubanite matrix. The identification of the two phases with different compositions determining the properties of the solid solution is an important result, which can facilitate the development of new magnetic sulfide nanomaterials and can be used for the processing of Cu-Fe sulfide ores.

Author contributions

I. G. Vasilyeva – methodology development, research concept, conducting research, text writing and editing, final conclusions. E. F. Sinyakova – methodology development, conducting experiments, results description, text editing. S. A. Gromilov – conducting X-ray diffraction analysis and interpreting the results, text writing.

Conflict of interests

The authors declare that they have no known competing financial interests or personal relationships that could have influenced the work reported in this paper.

References

1. Lyubutin I. S., Lin C.-R., Starchikov S. S., ... Wang S.-C. Synthesis, structural and magnetic properties of self-organized single-crystalline nanobricks of chalcopyrite $CuFeS_2$. *Acta Materialia*. 2013;61(11): 3956–3962. https://doi.org/10.1016/j.actamat.2013.03.009

2. Lyubutin I. S., Lin C.-R., Starchikov S. S., Siao Y.-J., Tseng Y.-T. Synthesis, structural and electronic properties of monodispersed self-organized single crystalline nanobricks of isocubanite $CuFe_2S_3$. *Journal of Solid State Chemistry*. 2015;221: 184–190. https://doi.org/10.1016/j.jssc.2014.10.006

3. Starchikov S. S. *Magnetic, structural and electronic properties of nanoparticles of iron sulfides and oxides with different crystal structure*[*]. Cand. of (phys.–math.) sci. diss. Abstr. Moscow: Nauka Publ.; 2015. 18 p. (In Russ.). Available at: https://www.crys.ras.ru/dissertations/Starchikov/Starchikov_avtoref.pdf

4. Putnis A., McConnel J. D. C. *Principle of mineral behavior*. Oxford-London-Edinburg-Boston-Melbourne: Blackwell Scientific Publications; 1980, 272 p.

5. Vaughan D. J., Craig J. R. *Mineral chemistry of metal sulfides*. Cambridge, UK: Cambridge Earth Science Series; Cambridge University Press: 1978, 493 p.

6. Sulfide mineralogy and geochemistry. D. J. Vaughan (ed.), Volume 61 in the series *Reviews in Mineralogy & Geochemistry*. https://doi.org/10.1515/9781501509490

7. Berger E. L., Keller L. P., Lauretta D. S. An experimental study of the formation of cubanite ($CuFe_2S_3$) in primitive meteorites. *Meteoritics and Planetary Science*. 2015;50: 1–14. https://doi.org/10.1111/maps.12399

8. Cabri L. J., Hall S. R., Szymanski J. T., Stewart J. M. On the transformation of cubanite. *Canadian Mineralogist*. 1973;12: 33–38.

9. René C., Cervelle B., Cesbron F., Oudin E., Picot P., Pillard F. Isocubanite, a new definition of the cubic polymorph of cubanite $CuFe_2S_3$. *Mineralogical Magazine*. 1988;52: 509–514. https://doi.org/10.1180/minmag.1988.052.367.10

10. Yund R. A., Kullerud G. Thermal stability of assemblages in the Cu-Fe-S system. *Journal of Petrology*. 1966;7: 454 – 488. https://doi.org/10.1093/petrology/7.3.454

11. Pruseth K. L., Mishra B., Bernhardt H. J. An experimental study on cubanite irreversibility: implications for natural chalcopyrite–cubanite intergrowths. *European Journal of Mineralogy*. 1999;11(3): 471–476. https://doi.org/10.1127/ejm/11/3/0471

12. Putnis A., McConnel J. D. C. The transformation behavior of metal-enriched chalcopyrite. *Contributions of Mineralogy and Petrology*. 1976;58: 127–136. https://doi.org/10.1007/bf00382181

13. Putnis A. Talnakhite and Mooihoekite: the accessibility of ordered structures in the metal-rich region around chalcopyrite. *Canadian Mineralogist*. 1978;16: 23–30.

14. Engin T. E., Powel A. B, Hull S. A high temperature diffraction-resistance study of chalcopyrite $CuFeS_2$. *Journal of Solid State Chemistry*. 2011;184: 2272–2277. https://doi.org/10.1016/j.jssc.2011.06.036

15. Putnis A. Electron microscope study of phase transformations in cubanite. *Physics and Chemistry of Minerals*. 1977;1: 335–349. https://doi.org/10.1007/bf00308844

16. Kosyakov V. I. Possible usage of directional crystallization for solving petrological problems. *Russian Geology and Geophysics*. 1998;39(9): 1245–1256.

17. Kosyakov V. I, Sinyakova E. F. Directional crystallization of Fe–Ni sulfide melts within the crystallization field of monosulfide solid solution. *Geochemistry International*. 2005;43(4): 372–85.

18. Kosyakov V. I., Sinyakova E.F. Melt crystallization of $CuFe_2S_3$ in the Cu–Fe–S system. *Journal of Thermal Analysis and Calorimetry*.2014;115: 511-516. https://doi.org/10.1007/s10973-013-3206-0

19. Kosyakov V. I., Sinyakova E. F. A. Study of crystallization of nonstoichiometric isocubanite $Cu_{1.1}Fe_{2.0}S_{3.0}$ from melt in the system Cu–Fe–S. *Journal of Thermal Analysis and Calorimetry*. 2017;129(2): 623–628. https://doi.org/10.1007/s10973-017-6215-6

20. Vasilyeva I. G., Sinyakova E. F., Gromilov S. A. Structural and chemical transformations of isocubanite $CuFe_2S_3$ at cooling from melt*. *Journal of Structural Chemistry = Zhurnal Strukturnoi Khimii*. 2024;65: 127132. (In Russ.). https://doi.org/10.26902/jsc_id127132

21. Malakhov V. V., Vasilyeva I. G. Stoichiography and chemical methods of phase analysis of multielement multiphase substances and materials. *Russian Chemical Reviews*. 2008;77(4): 351–372. https://doi.org/10.1070/RC2008v077n04ABEH003737

22. Malakhov V. V., Vasilyeva I. G. Stoichiography: evolution of solid-phase reactions. New principles of research, preparation and characterization of functional materials*. Novosibirsk: Siberian Branch of Russian Academy of Sciences Publ.; 2023. 251 c. (In Russ.)

23. Inorganic crystal structure database. D–1754. Eggenstein–Leopoldshafen: Germany. 2022.

24. Kraus W., Nolze G. POWDER CELL – a program for the representation and manipulation of crystal structures and calculation of the resulting X-ray powder patterns. *Journal of Applied Crystallography*. 1996;29: 301–303. https://doi.org/10.1107/s0021889895014920

25. Cabri L. J., Hall S. R., Szymanski J. T., Stewart J. M. On the transformation of cubanite. *Canadian Minerologist*. 1973;12: 33–38.

26. Dutrizac J. E. Reactions in cubanite and chalcopyrite. *Canadian Minerologist*. 1976; 14, 172–18

** Translated by author of the article*

Information about the authors

Inga G. Vasilyeva, Dr. Sci. (Chem.), Leading Research Fellow of Nikolaev Institute of Inorganic Chemistry Siberian Branch of RAS (NIIC SB RAS) (Novosibirsk, Russian Federation).

https://orcid.org/0000-0003-4045-9820

kamars@niic.nsc.ru

Elena F. Sinyakova, Dr. Sci. (Geol.–Min.), Leading Research Fellow of Sobolev Institute of Geology and Mineralogy of SB RAS (Novosibirsk, Russian Federation).

https://orcid.org/0000-0001-6288-3425

efsin@igm.nsc.ru

Sergey A. Gromilov, Dr. Sci. (Phys.–Math.), Leading Research Fellow, Nikolaev Institute of Inorganic Chemistry Siberian Branch of RAS (Novosibirsk, Russian Federation).

https://orcid.org/0000-0003-1993-5159

grom@niic.nsc.ru

Received 21.06.2024; approved after reviewing 31.07.2024; accepted for publication 16.09.2024; published online 25.12.2024.

Translated Yulia Dymant